Schwann cell-specific PTEN and EGFR dysfunctions affect neuromuscular junction development by impaired Agrin signaling and autophagy

Shi-Jie Zhang,[1, 2, 3, 5], Xiao-Xiao Li[1, 5], Yuyu Yu [1], Amy P. Chiu[1], Lilian H. Lo[1], Jeffrey C. To[1], Dewi K. Rowlands[4], Vincent W. Keng[1, *]

[1]Department of Applied Biology and Chemical Technology, The Hong Kong Polytechnic University, Kowloon, Hong Kong SAR.

[2]Department of Neurology, Second Affiliated Hospital of Guangzhou University of Chinese Medicine, Guangzhou, China.

[3]Institute of Clinical Pharmacology, Guangzhou University of Chinese Medicine, Guangzhou, China.

[4]Laboratory Animal Services Centre, The Chinese University of Hong Kong, Sha Tin, New Territories, Hong Kong SAR.

[5]These authors contribute equally.

[*] **Correspondence: vincent.keng@polyu.edu.hk**

Vincent W. Keng

Email: vincent.keng@polyu.edu.hk

Telephone: +852-3400-8728

Fax: +852-2364-9932

Abstract

The neuromuscular junction (NMJ) is formed by motor nerve terminals, post-junctional muscle membranes, and terminal Schwann cells (SCs). The formation of NMJ requires complex and dynamic molecular interactions. Nerve- and muscle-derived molecules have been well characterized but the mechanistic involvement of SC in NMJ development remains poorly understood. Schwann cell-specific *phosphatase and tensin homolog (Pten)* inactivation and *epidermal growth factor receptor (EGFR)* overexpression (*Dhh*-Cre; *Cnp-EGFR*; *Pten*$^{flox/flox}$ or DET) mice were used to study. In this study, NMJ malformation was observed in DET mice. Acetylcholine receptors (AChRs) were distorted and varicose presynaptic nerve terminals appeared in the tibialis anterior (TA) muscle of DET mice. Agrin signaling, related to NMJ development, was down-regulated in TA muscle. For mechanism study, both RAS/MEK/ERK and PI3K/AKT/mTOR signaling pathways were activated in the sciatic nerves of DET mice. Besides, autophagy was downregulated in these sciatic nerves. Torin 2, an mTOR inhibitor, rescued these phenotypes. The downregulated-autophagy might result in Agrin signaling abnormity, which induced NMJ malformation. Taken together, our results indicate that SCs-specific Pten and EGFR are critical for NMJ development.

Key words: Neuromuscular junction; Schwann cells; Pten; EGFR

Abbreviations: PNS, peripheral nervous systems; CNS, central nervous systems; SCs, schwann cells; NMJ, neuromuscular junction; AChRs, acetylcholine receptors; *PTEN, phosphatase and tensin homolog*; EGFR, epidermal growth factor receptor; MPNSTs, malignant peripheral nerve sheath tumors; TA, tibialis anterior; TEM, Transmission electron microscopy; *Rps20, ribosomal protein S20*; *Dmd, dystrophin, muscular dystrophy*; *Lamb2, laminin, beta 2*; *Chrna1, cholinergic receptor, nicotinic, alpha polypeptide 1*; *Dag1, dystroglycan 1*; DGC, dystrophin-glycoprotein complex.

Introduction

During muscle development and movement in vertebrates, peripheral and central nervous systems (PNS and CNS, respectively) participate in the progress through motor neuron axons [1]. Motor neuron axons stretch out from the spinal cord to the muscle fibers. The direction and integrity of these axons depend not only on neuron-derived interactions among axons, but also on the support from axonal Schwann cells (SCs) [2]. Motor axons are long structures that link to specific muscles, with the neuromuscular junction (NMJ) acting as a bridge between the nervous system and the muscular system. NMJ is a tripartite synapse, including motor nerve terminals, muscular post-junctional membranes and SCs that cover the entire nerve-muscle junction [3]. Axons release acetylcholine, which can bind to acetylcholine receptors (AChRs) located on the muscle fibers. In response to innervation of nerve terminals, these receptors are aggregated on the muscle fibers. The intimate interaction between motoneurons and skeletal muscle fibers induces NMJ formation with its abnormal development results in neurological muscular disorders [4]. Complex signal processes of NMJ development are necessary for muscular function. Agrin, a component of extracellular matrix, is required for nerve induction of AChR clustering [5]. Both LRP4-MuSK signaling [6] and Hippo pathways [7] are involved in the Agrin-mediated NMJ development.

Recently, SCs has created great attention in NMJ development, but the actual mechanism remains elusive. SCs can sense nerve-released acetylcholine and in turn influence transmitter release [8]. SCs can also regulate synapse elimination during

NMJ formation [9]. After injury, SCs guide the regenerated motor axons to the original site of innervation [10]. Nerve terminal growth and AChR clusters were shown to be reduced after ablation of SCs [11]. In addition, terminal SCs ablation can induce NMJ withdrawal and fragmentation [12]. At the molecular level, NMJ deficits were observed in SCs-specific *Nrg1* and *Erbb2* mutant mice [13].

The *phosphatase and tensin homolog* (*PTEN*) tumor suppressor gene, regulates cell growth and survival through inhibition of the PI3K/AKT/mTOR pathway. Previous study has found that genetically disrupting PTEN in SCs can markedly delay onset of both developmental myelination and remyelination after injury[14]. In Schwann cells, DLG1 interacts with PTEN to inhibit axonal stimulation of myelination [15]. The epidermal growth factor receptor (EGFR) is a receptor for members of the epidermal growth factor family of extracellular protein ligands. The functional role of EGFR signaling in myelination has been reported by both gain- and loss-of-function approaches [16]. However, the roles of PTEN and EGFR in NMJ development remain to be elucidated.

We have previously established a mouse model that generates sporadic malignant peripheral nerve sheath tumors (MPNSTs) by *Pten* inactivation and *EGFR* overexpression in Schwann cells[17]. While investigating MPNSTs in this mouse model, we serendipitously found that the muscle was remarkably weak in postnatal experimental animals. Further analyses of this phenotype revealed the SCs-specific role of *Pten* and *EGFR* in NMJ development.

Material and methods

Generation of experimental animals

For Schwann cell-specific *Pten* ablation, *Pten*$^{flox/flox}$ mice were crossed to desert hedgehog (*Dhh*)-Cre transgenic mice to obtain *Dhh*-Cre; *Pten*$^{flox/+}$ mice. Transgenic mice carrying the floxed *Pten* allele have the essential exons 4 and 5 of the *Pten* gene floxed with loxP sequences. For Schwann cell-specific *EGFR* overexpression, transgenic mice carried the *2',3'-cyclic nucleotide 3' phosphodiesterase* (*Cnp*) gene regulatory element driving human EGFR gene (*Cnp-EGFR*). *Cnp-EGFR* mice were crossed with *Pten*$^{flox/flox}$ mice to obtain *Cnp-EGFR*; *Pten*$^{flox/+}$ mice. Finally, *Dhh*-Cre; *Pten*$^{flox/+}$ mice were crossed with *Cnp-EGFR*; *Pten*$^{flox/+}$ mice to obtain the Schwann cell-specific *Pten* inactivation and *EGFR* overexpression (*Dhh*-Cre; *Cnp-EGFR*; *Pten*$^{flox/flox}$ or DET) mice. Genotyping was performed as described previously (**Supplement Fig. 1**) [17]. Experimental animals were sacrificed on postnatal days (P) 10, P20 and P30 for analyses. All animal studies were approved by the appropriate ethics committee and performed in accordance with the ethical standards stipulated by both The Hong Kong Polytechnic University and The Chinese University of Hong Kong.

Histological analyses

Tibialis anterior (TA) muscles were collected from experimental mice after euthanization by carbon dioxide. TA muscles were fixed in 10 % formalin, embedded into paraffin and sectioned for further histological analyses. Hematoxylin and eosin staining of mouse TA muscle sections was performed using standard procedures.

Transmission electron microscopy (TEM) analyses

TEM analysis of TA muscles was performed as described previously [18]. Ultrathin sections were cut and then stained with lead citrate before imaging using a transmission electron microscope (Philips CM100 TEM, Electron microscope unit, The University of Hong Kong).

Confocal microscope analyses

TA muscles were freshly dissected from mice and fixed overnight in 4 % PFA, rinsed with PBS before incubated with 0.1M glycine in PBS for one hour at room temperature. After rinsing with 0.5 % Triton X-100 in PBS, muscles fibers were incubated in blocking buffer (5% BSA and 1% Triton X-100 in PBS) for one hour. Tissues were then incubated with the following antibodies overnight: anti-neurofilament 200kDA, clone NE14, Alexa Fluor 555 conjugate (1:500, Merck Millipore Sigma, Massachusetts, USA), alpha-bungarotoxin, Alexa Fluor 488 conjugate (1:200, Thermo Fisher Scientific, Massachusetts, USA). Images were collected using flurescence microscope (Leica TCS SP8 Multiphoton Microscope, University Life Science, The Hong Kong polytechnic University).

Quantitative PCR (qPCR) analyses

Total RNA was extracted from frozen TA muscles using the RNAeasy Micro kit (Qiagen, Hilden, Germany) according to the manufacturer's recommendations and qPCR was performed as previously described [19] using the StepOnePlus Real-Time PCR System (Life Technologies, California, USA). Expression data were normalized to *ribosomal protein S20* (*Rps20*) expression. Primers sequences were as follows: *Rps20* forward, 5'-TGCTGAGGAACAAGTCGGTC-3' and *Rps20* reverse,

5’-AGTCCGCACAAACCTTCTCC-3’; *dystrophin, muscular dystrophy* (*Dmd*) forward 5’-CTCACTGCCTGTGAAACCCT-3’ and *Dmd* reverse, 5’-CAGGCTCAAGAGATCCAAGCA-3’; *laminin, beta 2* (*Lamb2*) forward, 5’-ACCCACACGGTCGGGATG-3’ and *Lamb2* reverse, 5’-ACAGCCAGGTACATCCAAGG-3’; *Agrn* forward, 5’-CTAGGGGAATCTCCGGTCCC-3’ and *Agrn* reverse, 5’-CCCATTAAGGCAGGGGTTGT-3’; *cholinergic receptor, nicotinic, alpha polypeptide 1* (*Chrna1*) forward, 5’-TATAACAACGCAGACGGCGA-3’ and *Chrna1* forward, 5’-GCTGGTCACTTTCCGGGTTA; *dystroglycan 1* (*Dag1*) forward, 5’-GAGGGACTGGAAGAACCAGC-3’ and *Dag1* reverse, 5’-CCTGCTGCAGACACCTTGAT-3’.

Western blot analyses

Sciatic nerves were homogenized and lysed with sodium dodecyl sulphate lysis buffer. The lysate was fractionated by SDS-polyacrylamide gel electrophoresis and then transferred onto polyvinylidene fluoride membranes. Primary antibodies used for immunoblotting were as follows: anti-phosphatidylinositide 3-kinases p85 (PI3K) (1:2000, Cell Signaling Technology, Massachusetts, USA); anti-phospho-PI3K p85 (Tyr458) (p-PI3K, 1:2000, Cell Signaling Technology); anti-phospho-AKT (Ser473) (p-AKT, 1:2000, Cell Signaling); anti-AKT (1:2000, Cell Signaling Technology); anti-phospho-ERK 1/2 (Thr202/Tyr204) (p-ERK, 1:2000, Cell Signaling Technology); anti-ERK 1/2 (1:2000, Cell Signaling Technology); anti-p62 (1 : 2000, Cell Signaling Technology); autophagy marker anti-LC3B (1:1000, Cell Signaling Technology);

anti-phospho-mammalian target of rapamycin complex 1 (p-mTOR, Ser2448) (1:1000, Cell Signaling Technology). The membranes were then incubated with secondary antibody (anti-rabbit or anti-mouse). Protein loading was detected by using super-enhanced chemiluminescence reagent (Merck Millipore Sigma).

Treatment of mice with mTOR inhibitor

Intraperitoneal injections of Torin 2 (MedChemExpress, New Jersey, USA) at 4 mg/kg/day were performed. DET mice received Torin 2 or only the carrier solution as a control from birth up to 3-month. Mortality of mice was recorded.

Rotarod performance test

The experimental procedure was performed as described previously[20]. Briefly, each experimental mouse (P30) was given 3 trials of walking in the rotating roll until they drop down, and the time of latency to fall was recorded. The apparatus used was LE8200 (Panlab, Harvard Apparatus).

Statistical analysis

The number of animals used for each experiments and analysis used in each panel are stated in the figure legends. All bar graphs represent mean ± SEM and all statistical analyses were performed using GraphPad (California, USA) Prism software (v6). The two-tailed Student's t-test was used for group comparisons and were considered statistically significant if $P < 0.05$.

Results

Muscular dysplasia in Schwann cell-specific *Pten* inactivation and *EGFR* overexpression (DET) mice

We first noticed that the DET mice displayed runty phenotype with tremoring, difficulty in movement. In contrast, experimental groups including: wild-type (WT), (2) *Dhh*-Cre only, (3) *Cnp-EGFR* only, (4) *Dhh*-Cre; *Pten* $^{f/f}$, (5) *Dhh*-Cre; *Pten* $^{f/+}$; *Cnp-EGFR*, all looked normal under the same conditions (*data not shown*). P10, P20 and P30 mice were used to study the different development stages of the muscular dysplasia. Both the average body weight and height of DET mice were significantly less than that in the other three groups (*Dhh*-Cre only, *Cnp-EGFR* only and *Dhh*-Cre; *Pten* $^{f/f}$) at P10, P20 and P30 (**Fig. 1A** to **F**). These data indicated that the muscle development of DET mice was delayed from an early postnatal age. TA muscle from P30 DET mice were used for further study and compared with *Dhh*-Cre mice (*Dhh* $^{Tg/+}$) as control. Histological analyses of TA muscle by HE staining showed altered fiber density or smaller fiber shape in DET mice when compared with control (**Fig. 1G**). Furthermore, TEM studies of TA muscle from P30 DET mice showed abnormal ultrastructural organization with narrow sarcomeres and partially distorted Z-lines, while TA muscle from the control group was consistently well-organized (**Fig. 1H**). Based on these analyses, it could be concluded that muscular dysplasia occurred in DET mice.

Morphological alterations of NMJ in DET mice

Since NMJ acts as a bridge between axons and muscle, it was hypothesized that the muscular dysplasia was caused by NMJ dysfunction in DET mice. TA muscle fibers from P30 DET mice were probed with antibody against neurofilament to label axons and alpha-bungarotoxin to label AChRs. The morphology of post-synaptic

AChRs, which indicates the endplate development of NMJ, in DET mice were abnormal, with distorted round shape endplates and perforated endplates, suggesting a delayed endplate maturation phenotype. In contrast, the AChRs in control group looked structurally consistent, with mature branched endplates distributed (**Fig. 2A-D**). Besides, a significant decrease in the mRNA level of *Chrna1* was also evident in DET mice (**Fig. 2E**).

Impaired Agrin signaling in NMJ development of DET mice

Synaptic basal lamina, a form of extracellular matrix, together with *Agrn* and *Lamb2*, are essential for NMJ formation and maintenance [21]. Significantly decreased mRNA levels of *Agrn* and *Lamb2* were evident in DET mice when compared with control group (**Fig. 3A** and **B**). Agrn triggers myocyte proliferation by modulation of dystrophin-glycoprotein complex (DGC) signaling. ECM-DGC interaction through Dag1 promotes myocyte differentiation and maturation. Dag1 also serves as a receptor for Agrn [22]. The mRNA level of *Dag1* was significantly decreased in DET mice when compared with control group (**Fig. 3C**). It has been previously shown that mice lacking *Dmd* show muscle weakness at young ages[23]. In our study, the mRNA level of *Dmd* was also decreased in DET mice when compared with control group (**Fig. 3D**). These results indicated that the SC-specific mutation in DET mice induced NMJ malformation by impairing Agrin signaling.

SC-specific mTOR-autophagy pathway changed in DET mice

EGFR overexpression can result in upregulation of RAS/MEK/ERK signaling pathway [16]. An increased phosphorylation of MEK and ERK were detected in the

sciatic nerves of DET mice, indicating RAS/MEK/ERK signaling pathway activation (**Fig. 4A and B**). Both *Pten* inactivation and *EGFR* overexpression can activate the PI3K/AKT/mTOR signaling pathway [17]. In our study, we found increased phosphorylation of PI3K, AKT, mTOR in the sciatic nerves of DET mice, indicating PI3K/AKT/mTOR signaling pathway activation (**Fig. 4C-E**). In addition, the activation of ERK can also promote mTOR phosphorylation[24] and play a crucial role in regulating autophagy[25]. Thus, two autophagy markers, P62 and LC3B, were assessed in the sciatic nerves of DET mice by Western blot analyses. Results showed that P62 was upregulated and LC3B was downregulated in DET mice, indicating the inhibition of autophagy (**Fig. 4F** and **G**). To confirm the key role of mTOR in NMJ development, DET mice were treated with Torin 2, a drug that primarily inhibits mTOR signaling. Torin 2 reversed the muscle weakness, shown as increased running time in the rotarod test (**Fig. 4H**) and extended the lifespan (**Fig. 4I**) of DET mice. Therefore, upregulation of the mTOR pathway in SCs underlied the dysfunction of NMJ development in DET mice.

Discussion

Our results revealed that both *PTEN* and *EGFR* are crucial regulators of the mTOR/autophagy signaling pathway in SCs that influence NMJ development. Conditional inactivation of *Pten* with *EGFR* overexpression in SCs induces activation of both RAS/MEK/ERK and PI3K/AKT/mTOR signaling pathways, which resulted in the NMJ malformation at a young postnatal age. The hyperactivation of mTOR can inhibit autophagy, which plays an important role in NMJ development process, since

Torin 2 treatment effectively rescues this effect. Mice with either SC-specific *Pten*-deficiency or overexpression of *EGFR* do not display any NMJ phenotype at a young postnatal age. Taken together, these results revealed the importance of *Pten* and *EGFR* in SCs for NMJ formation.

Although synapse formation during the NMJ development has been well studied, the contribution of the glial cells, such as presynaptic SCs, to NMJ development remains unclear [26]. Recently, it has been shown that presynaptic SCs contribute to pre- and post-synaptic maturation [27]. Importantly, the molecular pathways in SCs that drive NMJ development are yet to be elucidated. SCs can release synaptogenic factors, promote synaptogenesis and regulate motoneurons [28]. Previously, the role of SCs in NMJ development was showed by studying *Nrg1* and *Erbb2* mutant mice [27]. In our study, inactivation of *Pten* with *EGFR* overexpression in SCs induced NMJ malformation as shown by the reduction of AChR cluster sizes and the appearance of varicose nerve terminals. Many studies have demonstrated the importance of Agrin signaling in NMJ formation [5,29,30]. Agrin modulates DGC integrity and signaling through Dag1, which induces AChR clustering in cultured muscles and direct NMJ formation [31]. Recent evidence indicates that Yap is required for the formation of NMJ, by tethering to DGC upon activation and Agrin signaling [7]. Since SCs can also release Agrin, this further supports the importance of Agrin signaling in NMJ formation in TA muscles [32].

PTEN is a tumor suppressor gene that plays an important role in regulating cell growth, survival and migration. In SCs, mammalian DLG1-PTEN interaction

regulates myelin thickness [15], while *PTEN* loss-of-function hampers myelination [14]. Synaptic remodeling has been shown to be related with myelinating SCs [33] and dysmyelinated motoneurons results in NMJ developmental defects [34]. These findings indicate that SCs-specific *PTEN* mutation might regulate NMJ development. Interestingly, we found no abnormality in P30 SC-specific *Pten*-mutated mice. *EGFR* is a receptor for members of the EGF family of extracellular protein ligands. Activation of *EGFR* can promote cell proliferation, migration, adhesion, angiogenesis, and inhibition of apoptosis [35]. EGFR signaling in SCs can mediate myelination and remyelination [16]. We also did not observe muscle weakness in P30 *EGFR*-overexpressing mice. However, when inactivation of *Pten* and *EGFR* overexpression were concurrence in SCs, dysregulation of NMJ development occurred. The molecular pathways involved the upregulation of both RAS/MAPK/ERK and PI3K/AKT/mTOR signaling pathways, consistent with our previous report [17]. Upregulation of RAS/MAPK/ERK or PI3K/AKT/mTOR signaling pathway alone did not affect NMJ development at a young postnatal age. Since activation of ERK can also promote mTOR phosphorylation [24], it is hypothesized that hyperactivation of mTOR might be the key factor in SCs-mediated NMJ dysfunction since previous study has shown that loss of mTOR function delayed SC myelination[36]. Activation of mTOR signaling results in axonal degeneration [37,38,39] and also plays a crucial role in regulating autophagy. Inhibition of SCs-specific autophagy results in abnormally enlarged abaxonal cytoplasm in myelinating SCs [40]. Torin 2, an mTOR inhibitor, rescued some of the phenotypes of

DET mice. These data indicate that the inactivation of PTEN with EGFR overexpression in SCs-induced NMJ malformation is largely dependent on mTOR-autophagy signaling.

Our study revealed the cooperation of RAS/MAPK/ERK and PI3K/AKT/mTOR signaling pathways in SCs may be an important contributing factor in regulating NMJ development, and closely associated with the mTOR-autophagy signaling pathway.

Conflicts of interest

None

Acknowledgement

This study was supported by Research Grants Council Collaborative Research Fund Scheme (C5012-15E), Hong Kong SAR Government; and the Department of Applied Biology and Chemical Technology, The Hong Kong Polytechnic University, Hong Kong SAR (G-YBTA).

References

[1] R. Mirsky, J. Gavrilovic, P. Bannerman, J. Winter, K.R. Jessen, Characterization of a plasma membrane protein present in non-myelin-forming PNS and CNS glia, a subpopulation of PNS neurons, perineurial cells and smooth muscle in adult rats, Cell Tissue Res 240 (1985) 723-733.

[2] A.F. Rosenberg, J. Isaacman-Beck, C. Franzini-Armstrong, M. Granato, Schwann cells and deleted in colorectal carcinoma direct regenerating motor axons towards their original path, J Neurosci 34 (2014) 14668-14681.

[3] C.P. Ko, R. Robitaille, Perisynaptic Schwann Cells at the Neuromuscular Synapse: Adaptable, Multitasking Glial Cells, Cold Spring Harb Perspect Biol 7 (2015).

[4] A.G. Engel, K. Ohno, S.M. Sine, Sleuthing molecular targets for neurological

diseases at the neuromuscular junction, Nat Rev Neurosci 4 (2003) 339-352.

[5] Y. Zong, B. Zhang, S. Gu, K. Lee, J. Zhou, G. Yao, D. Figueiredo, K. Perry, L. Mei, R. Jin, Structural basis of agrin-LRP4-MuSK signaling, Genes Dev 26 (2012) 247-258.

[6] Y. Zong, R. Jin, Structural mechanisms of the agrin-LRP4-MuSK signaling pathway in neuromuscular junction differentiation, Cell Mol Life Sci 70 (2013) 3077-3088.

[7] K. Zhao, C. Shen, Y. Lu, Z. Huang, L. Li, C.D. Rand, J. Pan, X.D. Sun, Z. Tan, H. Wang, G. Xing, Y. Cao, G. Hu, J. Zhou, W.C. Xiong, L. Mei, Muscle Yap Is a Regulator of Neuromuscular Junction Formation and Regeneration, J Neurosci 37 (2017) 3465-3477.

[8] R. Robitaille, Modulation of synaptic efficacy and synaptic depression by glial cells at the frog neuromuscular junction, Neuron 21 (1998) 847-855.

[9] J.C. Tapia, J.D. Wylie, N. Kasthuri, K.J. Hayworth, R. Schalek, D.R. Berger, C. Guatimosim, H.S. Seung, J.W. Lichtman, Pervasive synaptic branch removal in the mammalian neuromuscular system at birth, Neuron 74 (2012) 816-829.

[10] Q.T. Nguyen, J.R. Sanes, J.W. Lichtman, Pre-existing pathways promote precise projection patterns, Nat Neurosci 5 (2002) 861-867.

[11] L.V. Reddy, S. Koirala, Y. Sugiura, A.A. Herrera, C.P. Ko, Glial cells maintain synaptic structure and function and promote development of the neuromuscular junction in vivo, Neuron 40 (2003) 563-580.

[12] A. Barik, L. Li, A. Sathyamurthy, W.C. Xiong, L. Mei, Schwann Cells in Neuromuscular Junction Formation and Maintenance, J Neurosci 36 (2016) 9770-9781.

[13] L. Li, W.C. Xiong, L. Mei, Neuromuscular Junction Formation, Aging, and Disorders, Annu Rev Physiol 80 (2018) 159-188.

[14] G. Figlia, C. Norrmen, J.A. Pereira, D. Gerber, U. Suter, Dual function of the PI3K-Akt-mTORC1 axis in myelination of the peripheral nervous system, Elife 7 (2017) 29241.

[15] L. Cotter, M. Ozcelik, C. Jacob, J.A. Pereira, V. Locher, R. Baumann, J.B. Relvas,

U. Suter, N. Tricaud, Dlg1-PTEN interaction regulates myelin thickness to prevent damaging peripheral nerve overmyelination, Science 328 (2010) 1415-1418.

[16] A. Aguirre, J.L. Dupree, J.M. Mangin, V. Gallo, A functional role for EGFR signaling in myelination and remyelination, Nat Neurosci 10 (2007) 990-1002.

[17] V.W. Keng, A.L. Watson, E.P. Rahrmann, H. Li, B.R. Tschida, B.S. Moriarity, K. Choi, T.A. Rizvi, M.H. Collins, M.R. Wallace, N. Ratner, D.A. Largaespada, Conditional Inactivation of Pten with EGFR Overexpression in Schwann Cells Models Sporadic MPNST, Sarcoma 620834 (2012) 18.

[18] M.L. Bang, X. Li, R. Littlefield, S. Bremner, A. Thor, K.U. Knowlton, R.L. Lieber, J. Chen, Nebulin-deficient mice exhibit shorter thin filament lengths and reduced contractile function in skeletal muscle, J Cell Biol 173 (2006) 905-916.

[19] Y. Morikawa, M. Zhang, T. Heallen, J. Leach, G. Tao, Y. Xiao, Y. Bai, W. Li, J.T. Willerson, J.F. Martin, Actin cytoskeletal remodeling with protrusion formation is essential for heart regeneration in Hippo-deficient mice, Sci Signal 8 (2015) 2005781.

[20] H. Shiotsuki, K. Yoshimi, Y. Shimo, M. Funayama, Y. Takamatsu, K. Ikeda, R. Takahashi, S. Kitazawa, N. Hattori, A rotarod test for evaluation of motor skill learning, J Neurosci Methods 189 (2010) 180-185.

[21] H. Wu, W.C. Xiong, L. Mei, To build a synapse: signaling pathways in neuromuscular junction assembly, Development 137 (2010) 1017-1033.

[22] M.A. Bowe, K.A. Deyst, J.D. Leszyk, J.R. Fallon, Identification and purification of an agrin receptor from Torpedo postsynaptic membranes: a heteromeric complex related to the dystroglycans, Neuron 12 (1994) 1173-1180.

[23] C. Pisani, G. Strimpakos, F. Gabanella, M.G. Di Certo, A. Onori, C. Severini, S. Luvisetto, S. Farioli-Vecchioli, I. Carrozzo, A. Esposito, T. Canu, E. Mattei, N. Corbi, C. Passananti, Utrophin up-regulation by artificial transcription factors induces muscle rescue and impacts the neuromuscular junction in mdx mice, Biochim Biophys Acta 4 (2018) 31.

373 [24] M.C. Mendoza, E.E. Er, J. Blenis, The Ras-ERK and PI3K-mTOR pathways:
374 cross-talk and compensation, Trends Biochem Sci 36 (2011) 320-328.
375 [25] Y.C. Kim, K.L. Guan, mTOR: a pharmacologic target for autophagy regulation, J
376 Clin Invest 125 (2015) 25-32.
377 [26] C. Eroglu, B.A. Barres, Regulation of synaptic connectivity by glia, Nature 468
378 (2010) 223-231.
379 [27] H. Darabid, A.P. Perez-Gonzalez, R. Robitaille, Neuromuscular synaptogenesis:
380 coordinating partners with multiple functions, Nat Rev Neurosci 15 (2014)
381 703-718.
382 [28] H.B. Peng, J.-F. Yang, Z. Dai, C.W. Lee, H.W. Hung, Z.H. Feng, C.-P. Ko,
383 Differential effects of neurotrophins and schwann cell-derived signals on
384 neuronal survival/growth and synaptogenesis, Journal of Neuroscience 23
385 (2003) 5050-5060.
386 [29] T. Tezuka, A. Inoue, T. Hoshi, S.D. Weatherbee, R.W. Burgess, R. Ueta, Y.
387 Yamanashi, The MuSK activator agrin has a separate role essential for
388 postnatal maintenance of neuromuscular synapses, Proc Natl Acad Sci U S A
389 111 (2014) 16556-16561.
390 [30] M.A. Samuel, G. Valdez, J.C. Tapia, J.W. Lichtman, J.R. Sanes, Agrin and
391 synaptic laminin are required to maintain adult neuromuscular junctions, PLoS
392 One 7 (2012) 3.
393 [31] A. Barik, B. Zhang, G.S. Sohal, W.C. Xiong, L. Mei, Crosstalk between Agrin
394 and Wnt signaling pathways in development of vertebrate neuromuscular
395 junction, Dev Neurobiol 74 (2014) 828-838.
396 [32] J.F. Yang, G. Cao, S. Koirala, L.V. Reddy, C.P. Ko, Schwann cells express active
397 agrin and enhance aggregation of acetylcholine receptors on muscle fibers, J
398 Neurosci 21 (2001) 9572-9584.
399 [33] S.L. Roche, D.L. Sherman, K. Dissanayake, G. Soucy, A. Desmazieres, D.J.
400 Lamont, E. Peles, J.P. Julien, T.M. Wishart, R.R. Ribchester, P.J. Brophy, T.H.
401 Gillingwater, Loss of glial neurofascin155 delays developmental synapse
402 elimination at the neuromuscular junction, J Neurosci 34 (2014) 12904-12918.

[34] X. Yin, G.J. Kidd, E.P. Pioro, J. McDonough, R. Dutta, M.L. Feltri, L. Wrabetz, A. Messing, R.M. Wyatt, R.J. Balice-Gordon, B.D. Trapp, Dysmyelinated lower motor neurons retract and regenerate dysfunctional synaptic terminals, J Neurosci 24 (2004) 3890-3898.

[35] A.D. Durbin, D.H. Ki, S. He, A.T. Look, Malignant Peripheral Nerve Sheath Tumors, Adv Exp Med Biol 916 (2016) 495-530.

[36] C. Norrmen, G. Figlia, F. Lebrun-Julien, J.A. Pereira, M. Trotzmuller, H.C. Kofeler, V. Rantanen, C. Wessig, A.L. van Deijk, A.B. Smit, M.H. Verheijen, M.A. Ruegg, M.N. Hall, U. Suter, mTORC1 controls PNS myelination along the mTORC1-RXRgamma-SREBP-lipid biosynthesis axis in Schwann cells, Cell Rep 9 (2014) 646-660.

[37] B. Beirowski, E. Babetto, J.P. Golden, Y.J. Chen, K. Yang, R.W. Gross, G.J. Patti, J. Milbrandt, Metabolic regulator LKB1 is crucial for Schwann cell-mediated axon maintenance, Nat Neurosci 17 (2014) 1351-1361.

[38] C. Norrmen, U. Suter, Akt/mTOR signalling in myelination, Biochem Soc Trans 41 (2013) 944-950.

[39] G. Figlia, D. Gerber, U. Suter, Myelination and mTOR, Glia 66 (2018) 693-707.

[40] S.Y. Jang, Y.K. Shin, S.Y. Park, J.Y. Park, S.H. Rha, J.K. Kim, H.J. Lee, H.T. Park, Autophagy is involved in the reduction of myelinating Schwann cell cytoplasm during myelin maturation of the peripheral nerve, PLoS One 10 (2015).

Figure legends

Figure 1 Muscular dysplasia phenotype in Schwann cell-specific *Pten* inactivation and *EGFR* overexpressing (DET) mice. Body weights of postnatal day 10 (P10, **A**), P20 (**B**), P30 (**C**) mice from different genotypes. Body heights of P10 (**D**), P20 (**E**), P30 (**F**) mice from different genotypes. (**G**) Representative hematoxylin and eosin (HE) stained images of mouse TA muscle sections from DET mouse compared with *Dhh* $^{Tg/+}$ control. Scale bar, 10 μm. (**H**) Representative transmission electron microscopy analyses showing abnormal ultrastructural organization with narrow sarcomeres and partially distorted Z-lines (arrow) in DET TA muscles. Scale bar, 500 nm. Values were expressed as mean ± SEM. **P* < 0.05; ***P* < 0.01, compared with *Dhh* $^{Tg/+}$ control group.

Figure 2 Morphological alterations of *NMJ* in DET mice. (**A**) Representative confocal images of TA muscles taken from P30 control and DET mice. TA muscles were stained with antibodies against neurofilament Alexa Fluor 555 conjugate to label presynaptic axons (left panels), and alpha-bungarotoxin Alexa Fluor 488 conjugate to label AChR clusters (middle panels). Merged images from both stains shown in the right panels. Scale bar, 10 μm. Quantitative analyses of the AChR cluster size (**B**), AChR morphology (**C**) and NMJ innervation (**D**). (**E**) qPCR analysis of *Chrna1* expression in TA muscles taken from P30 control and DET mice. Values were expressed as mean ± SEM. **P* < 0.05, compared with *Dhh* $^{Tg/+}$ group.

Figure 3 Impaired Agrin signaling in NMJ development of DET mice. RNA was isolated from P30 hind limb muscles and analyzed for key genes involved with Agrin

signaling. Expression of (**A**) *Agrn*, (**B**) *Lamb2*, (**C**) *Dag1* and (**D**) *Dmd* were detected by qPCR. Values were expressed as mean ± SEM. **P* < 0.05; ***P* < 0.01, compared with *Dhh* $^{Tg/+}$ control group.

Figure 4 Activation of the mTOR-autophagic pathway in DET mice. (**A** to **G**) Western blot analyses were performed on sciatic nerves isolated from P30 control and DET mice to detect protein levels of p-MEK, p-ERK, p-PI3K, p-AKT, p-mTOR, P62 and LC3B (A-G). DET mice were treated with Torin 2 for 3 months, then assayed on the rotarod apparatus (**H**) and analyzed for its effect on survival (**I**). Values were expressed as mean ± SEM. **P* < 0.05; ***P* < 0.01, compared with *Dhh* $^{Tg/+}$ control.

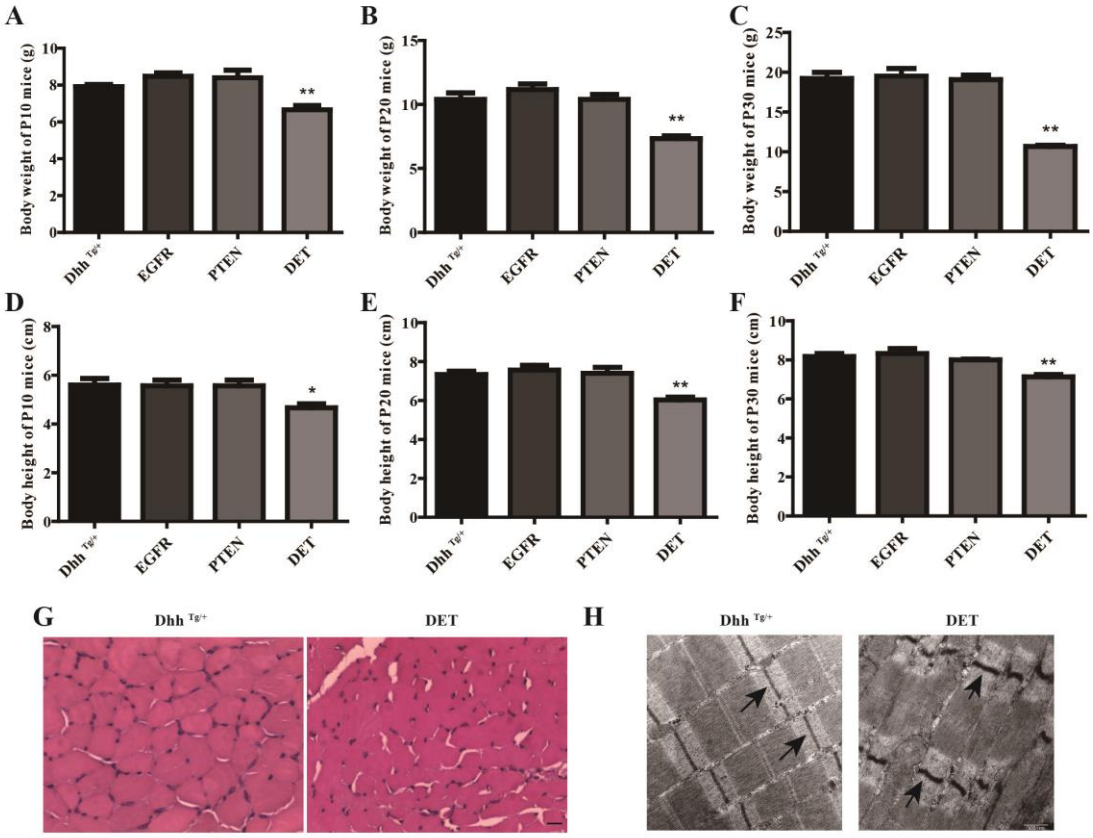
A
Body weight of P10 mice (g)
B
Body weight of P20 mice (g)
C
Body weight of P30 mice (g)
D
Body height of P10 mice (cm)
E
Body height of P20 mice (cm)
F
Body height of P30 mice (cm)
Dhh Tg/+
EGFR
PTEN
DET
G
H

460

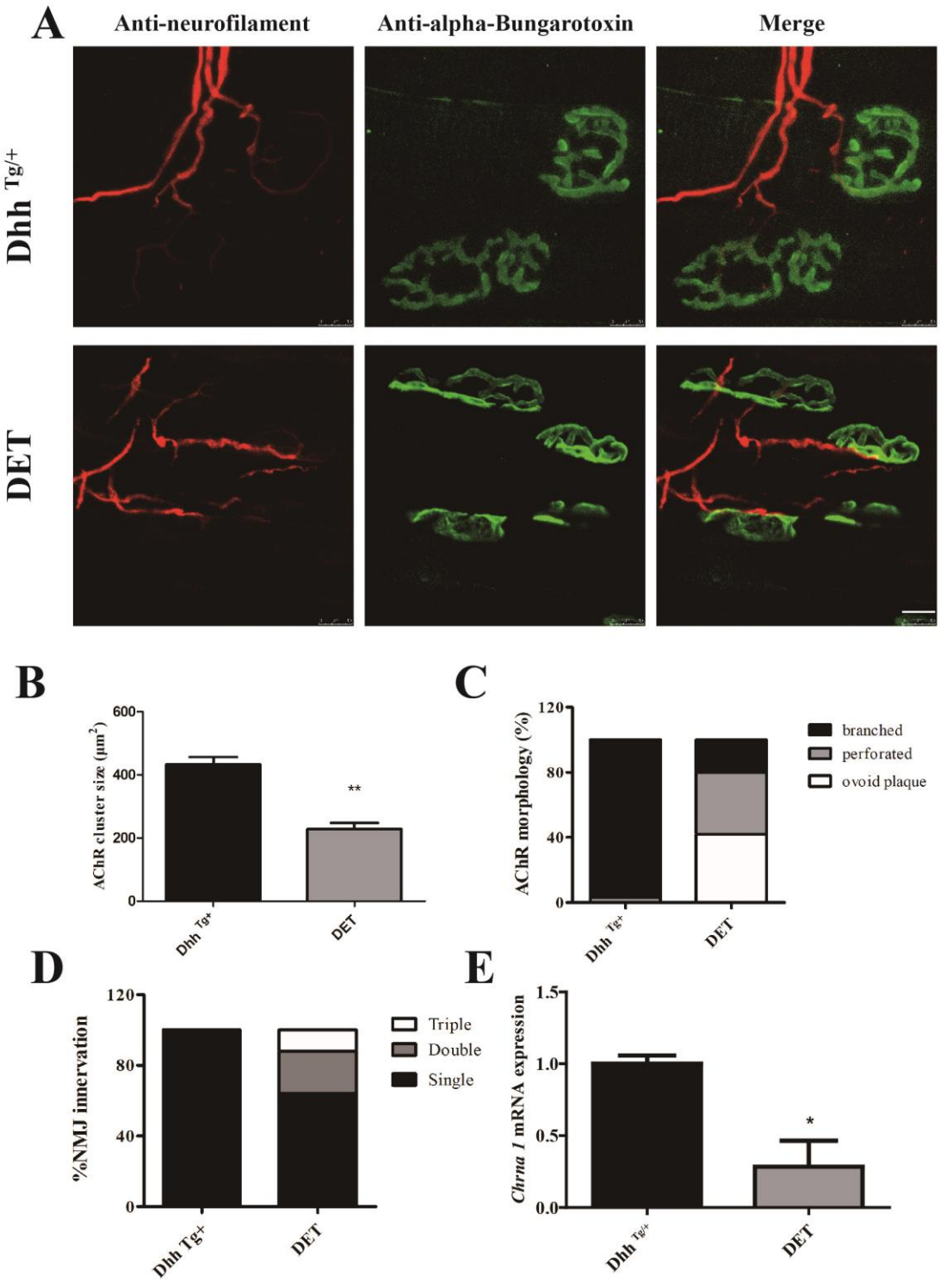
A
Anti-neurofilament
Anti-alpha-Bungarotoxin
Merge
Dhh Tg/+
DET
B
AChR cluster size (μm²)
600
400
200
0
**
Dhh Tg+
DET
C
AChR morphology (%)
120
80
40
0
branched
perforated
ovoid plaque
Dhh Tg+
DET
D
%NMJ innervation
120
80
40
0
Triple
Double
Single
Dhh Tg+
DET
E
Chrna 1 mRNA expression
1.5
1.0
0.5
0.0
*
Dhh Tg/+
DET

461

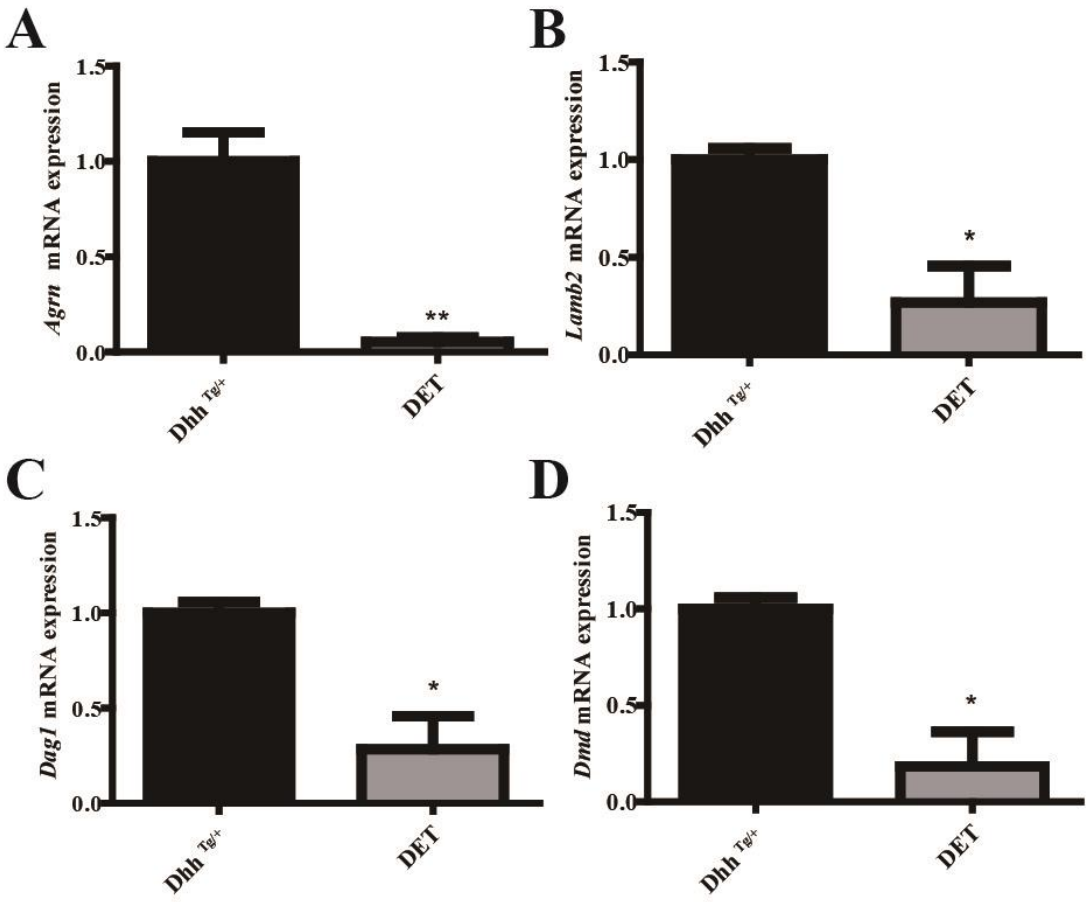
A
Agrn mRNA expression
1.5
1.0
0.5
0.0
**
Dhh Tg/+
DET
B
Lamb2 mRNA expression
1.5
1.0
0.5
0.0
*
Dhh Tg/+
DET
C
Dag1 mRNA expression
1.5
1.0
0.5
0.0
*
Dhh Tg/+
DET
D
Dmd mRNA expression
1.5
1.0
0.5
0.0
*
Dhh Tg/+
DET

462

463

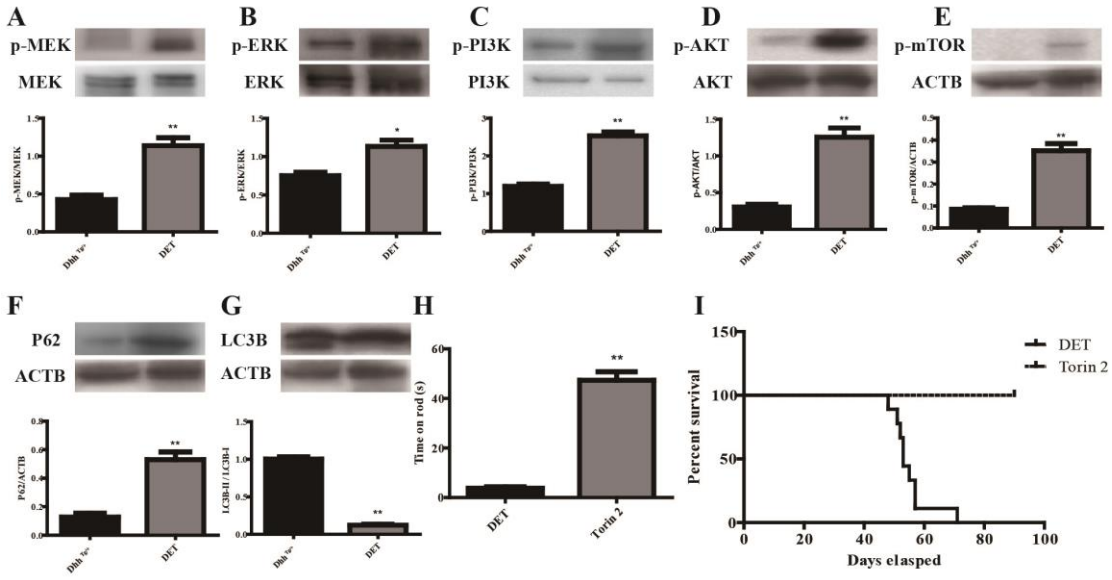
A
p-MEK
MEK
p-MEK/MEK
B
p-ERK
ERK
p-ERK/ERK
C
p-PI3K
PI3K
p-PI3K/PI3K
D
p-AKT
AKT
p-AKT/AKT
E
p-mTOR
ACTB
p-mTOR/ACTB
Dhh Tg+
DET
F
P62
ACTB
P62/ACTB
G
LC3B
ACTB
LC3B-II / LC3B-I
H
Time on rod (s)
DET
Torin 2
I
Percent survival
Days elasped
DET
Torin 2

464

465

466